Variability in sea ice carbonate chemistry: A case study comparing the importance of ikaite precipitation, bottom ice algae, and currents across an invisible polynya

Brent G. T. Else[1], Araleigh Cranch[1], Richard P. Sims[1,2], Samantha Jones[1], Laura A. Dalman[3,4], Christopher J. Mundy[3], Rebecca A. Segal[5,6], Randall K. Scharien[7], Tania Guha[1]

[1]Department of Geography, University of Calgary, Calgary, Alberta, Canada

[2]Now at: College of Life and Environmental Sciences, University of Exeter, Exeter, United Kingdom

[3]Centre for Earth Observation Science, University of Manitoba, Winnipeg, Manitoba, Canada

[4]Now at: Institute for Marine and Antarctic Studies, University of Tasmania, Hobart, Australia

[5]Arctic Eider Society, Sanikiluaq, Canada

[6]SmartIce Sea Ice Monitoring & Information Inc., St. John's, Canada

[7]Department of Geography, University of Victoria, Victoria, British Columbia, Canada

Correspondence to: Brent G. T. Else (belse@ucalgary.ca)

Abstract. The carbonate chemistry of sea ice is known to play a role in global carbon cycles, but its importance is uncertain in part due to disparities in reported results. Variability in physical and biological drivers is usually invoked to explain differences between studies. In the Canadian Arctic Archipelago, "invisible polynyas" – areas of strong currents, thin ice, and potentially high biological productivity – are examples of extreme spatial variability. We used an invisible polynya as a natural laboratory to study the effects of inferred initial ice formation conditions, ice growth rate, and algal biomass on the distribution of carbonate species by collecting enough cores to perform a statistical comparison between sites located within, and just outside of, a polynya near Iqaluktuttiaq (Cambridge Bay, Nunavut, Canada). At both sites, the uppermost 10-cm ice horizon showed evidence of CO_2 offgassing, while carbonate distributions in the middle and bottommost 10-cm horizons largely followed the salinity distribution. In the polynya, the upper-ice horizon had significantly higher bulk total inorganic carbon (TIC), total alkalinity (TA), and salinity, potentially due to freeze-up conditions that favoured frazil ice production. The middle-ice horizons were statistically indistinguishable between sites, suggesting that ice growth rate is not an important factor for the carbonate distribution under mid-winter conditions. The thicker (non-polynya) site experienced higher algal biomass, TIC, and TA in the bottom horizon. Carbonate chemistry in the bottom horizon could largely be explained by the salinity distribution, with the strong currents at the polynya site potentially playing a role in desalinisation; biology appeared to exert only a minor control, with some evidence that the ice algae community was net heterotrophic. We did see evidence of calcium carbonate precipitation, but with little impact on the TIC:TA ratio, and little difference between sites. Because differences were constrained to relatively thin layers at the top and bottom, vertically averaged values of TIC, TA, and especially the TIC:TA ratio were not meaningfully different between sites. This provides some justification for using a single bulk value for each parameter when modeling sea ice effects on ocean chemistry at coarse resolution. Exactly what value to use (particularly for the TIC:TA ratio) likely varies by region but could potentially be approximated from knowledge of the source seawater and sea ice salinity. Further insights await a rigorous intercomparison of existing data.

Deleted: be

Deleted: biology did not have a noticeable impact

1 Introduction

45 Polar seas typically act as strong sinks for atmospheric CO_2. Recent estimates of the Arctic CO_2 sink suggest an uptake on the order of 150-200 TgC year^{-1}, or about 10-14% of the global ocean sink (Bates and Mathis, 2009; Yasunaka et al., 2016; Manizza et al., 2019). This sink is significantly larger than one might expect given the relatively small surface area (about 3% of the global surface ocean). Carbon dioxide uptake for the sea ice zone of the Southern Ocean has been estimated at 56 TgC year^{-1} or about 50 4% of the global sink (Takahashi et al., 2009), slightly exceeding its relative surface area (3%).

The carbon sink in these polar regions is thought to be enhanced by some combination of the solubility pump (CO_2 is more soluble in cold water, and thus can be transported to depth by convection events), the biological pump (CO_2 sequestered in organic material is exported out of the surface ocean by sinking), and the "sea ice pump". The sea ice pump was first proposed by Rysgaard et al. (2007) who observed 55 elevated total alkalinity (TA) relative to total inorganic carbon (TIC) in melted sea ice samples. The hypothesized cause of this TA enrichment was the precipitation of ikaite, a calcium carbonate crystal form that has since been positively identified in Antarctic (Dieckmann et al., 2008) and Arctic (Dieckmann et al., 2010) sea ice. The theory posits that as sea ice grows and rejects impurities, ikaite crystals are formed and preferentially trapped in the sea ice matrix relative to brine. Ikaite is a form of 60 particulate inorganic carbon, but its precipitation lowers the TIC concentration of the source brine by only 1 mol while lowering TA by 2 mol. Brine that drains out of the ice during the desalination process (Notz and Worster, 2009) is therefore relatively enriched in dissolved inorganic carbon, leaving the bulk sea ice enriched in TA. If brines rich in dissolved inorganic carbon sink to sufficient depths, this sequesters carbon from the surface ocean, while the subsequent ice melt in spring releases TA to the surface ocean,

lowering pCO$_2$ and driving higher atmospheric CO$_2$ uptake during the open water season.

70   The fundamental parameter driving this pump is the TA:TIC ratio in sea ice, which if only affected by ikaite should range from 2:1 (the theoretical maximum ratio) to approximately 1:1 (seawater typically has a ratio near 1:1, which should be reflected in sea ice if brine is rejected conservatively). Published results have reported ratios spanning 0.9 to 2.2 from a variety of different Arctic and Antarctic field sites (Rysgaard et al., 2007, 2009; Miller et al., 2011a, 2011b; Geilfus et al., 2012; Brown et al., 2015; Findlay

75   et al., 2015). The absolute concentration values of TIC and TA in sea ice also span a significant range: for the above listed studies, these values range from <100 µmol kg^{-1} to >700 µmol kg^{-1} for both species. This observed variability suggests not only that ikaite precipitation is a variable process, but that other biogeochemical factors impact TIC and TA in sea ice.

Ice growth conditions are one set of factors that may affect sea ice carbonate chemistry. The physical

80   process of sea ice formation depends in part on turbulence (Martin and Kauffman, 1981; Savel'yev 1958, 1963). During initial ice formation, turbulent areas (driven by wind or tidal currents) generate large amounts of frazil ice in a thicker mixed layer, leading to a collision and bonding process that results in faster formation of floes (Martin and Kauffman, 1981; Chadian and Strickland-Constable, 1974; Chalmers and Williamson, 1965; Savel'yev 1958, 1963). In contrast, calmer areas develop thinner frazil

85   ice layers (Petrich & Eicken, 2010). Once the surface ice (approximately the first 30 cm or less) is consolidated, congelation (columnar) ice growth dominates, and the rate of growth strongly impacts brine rejection. Faster crystallization during sea ice formation typically results in increased retention of salts, including TIC. A laboratory study by König et al. (2018) found the amount of TIC trapped in sea ice almost doubled for sea ice grown at -40°C compared to ice grown at -15°C. In the natural environment,

90   ice growth rates are controlled not only by atmospheric forcing, but also by snow depth (deep snow

insulates the ice and lowers the growth rate) and under ice seawater temperature and currents (strong currents enhance ocean heat flux and lower the ice growth rate).

Gas exchange between the sea ice and the overlying atmosphere can also play a role in sea ice carbonate chemistry, at least in the upper layers of the ice. During ice formation, some brine is rejected upwards, allowing CO_2 to offgass to the atmosphere (Geilfus et al., 2013; Nomura et al., 2014). In the frazil crystal structures of surface ice, the high brine fraction creates high enough permeability (relative to layers immediately below it) for this outgassing to occur over a layer several centimetres thick (Moreau et al., 2015). Laboratory estimates have found that the amount of carbon released to the atmosphere via this process is a small fraction (<1%) of the total inorganic carbon redistributed by ice formation (Rysgaard et al., 2009; König et al, 2018). While gas exchange may not impact the entire ice column, it may be important in determining the vertical distribution of TIC in the surface horizon of the sea ice.

Biological processes are also likely to affect the vertical distribution of TIC and TA in sea ice. Miller et al. (2011a) found evidence for the production of CO_2 throughout the sea ice column in winter, likely as a result of respiration within brine inclusions. In the spring, algal blooms occur within the bottom of sea ice in many Arctic locations (Leu et al., 2015) and throughout the ice profile in Antarctic regions (e.g., Meiners et al., 2012, 2018), resulting in observed decreases in TIC in the lower horizons of sea ice cores (Dellile et al., 2007; Miller et al. 2011a; Brown et al., 2015). The spatial distribution of ice algae is known to be highly heterogeneous (Leu et al., 2015), contributing to high heterogeneity in other biogeochemical properties, including carbonate chemistry (Miller et al., 2015). In general, ice algal biomass is controlled by light availability (largely a function of snow cover, with thick snow reducing light transmission and ice algae production, e.g., Campbell et al. (2014)) and nutrient availability (potentially a function of

seawater nutrient concentration and turbulence, with strong currents enhancing nutrient supply and ice algal production, e.g., Dalman et al. (2019)).

The horizontal and vertical variability in sea ice TIC and TA that results from these processes may impact the efficiency of the sea ice carbon pump. In an early study, Rysgaard et al. (2011) used a simple box model and estimated its impact on air-sea CO_2 uptake to be 31 TgC year^{-1} in the Arctic and 52 TgC year^{-1} in the Antarctic. However, subsequent efforts using coupled 3-dimensional general circulation models produced much lower estimates. Grimm et al. (2016) found an enhancement of only 2-14 TgC year^{-1} for the Arctic and Antarctic Sea ice zones combined, while Moreau et al. (2016) attributed only a 4 TgC year^{-1} uptake globally to the sea ice pump. Using a one-dimensional model with more detailed biogeochemical processes, Mortenson et al. (2018) similarly found that ikaite precipitation and dissolution did not have a large impact on annual air-sea CO_2 flux budgets due to a lack of deep convection at their study site. However, both Grimm et al. (2016) and Moreau et al. (2016) concluded that the sea ice carbon pump is important in specific polar regions (most notably in deep water formation areas), and could be important on long timescales (e.g., during the glacial/interglacial transitions).

In sensitivity analyses, both Mortenson et al. (2018) and Grimm et al. (2016) found that the strength of the sea ice pump responds strongly to the prescribed TA:TIC ratio. Furthermore, Grimm et al. (2016) found that the absolute concentration of TA and TIC had a significant impact. It is also important to consider that all these studies were working from limited field data. Despite this sensitivity, and the observed variability in sea ice carbonate chemistry described above, the central results of most modeling studies use a single value for TIC, typically around 400 µmol kg^{-1}, and a single TA:TIC ratio, typically 2:1 (Rysgaard et al., 2011; Grimm et al., 2016; Mortenson et al., 2018).

If the biogeochemical processes responsible for variability in sea ice carbon system parameters can be

constrained by field measurements, that variability could conceivably be included in biogeochemical models, leading to better estimates of the role of the sea ice carbon pump in regional and global models.

150   Accordingly, this paper describes field measurements of TA and TIC in landfast first year sea ice cores collected at two sites in the Canadian Arctic Archipelago. The sites (separated by only 7 km) were chosen based on prior knowledge of significantly different physical and biological conditions due to the presence of an "invisible polynya" (Dalman et al., 2019) – a region of distinctly thinner ice within the landfast icescape (Melling et al., 2015). This paper seeks to contrast the two sites with objectives to characterize

155   how differing physical and biological processes impact both horizontal and vertical distributions of carbonate properties in sea ice and determine if these processes affect the bulk estimates of TA and TIC commonly ingested into models of the sea ice carbon pump.

2 Methods

2.1 Study area

160   This study was conducted in Dease Strait, a narrow channel that is part of the southern limb of the Northwest Passage in the Canadian Arctic Archipelago. In the winter, Dease Strait is covered by landfast first-year sea ice that typically consolidates in early November, and breaks up in mid-July (Galley et al., 2012, Xu et al., 2021). The strait is relatively shallow (max depth ~100 m), and surface waters are somewhat less saline (~29) than most of the Archipelago due to high river discharge and

165   bounding sills to the east and west (Williams et al., 2018; Xu et al., 2021). The region is severely nutrient limited, with nitrate concentrations amongst the lowest measured anywhere in the Arctic ($1.0 – 1.2$ μmol L^{-1} beneath the pycnocline in summer (Back et al., 2021); 1.3 μmol L-1 beneath sea ice

(Dalman et al., 2019)). However, a modest bottom-ice algae bloom still occurs in the spring, peaking in late-May (Campbell et al., 2016).

Our sites were located near the Finlayson Islands, a chain of rocky outcrops about 30 km west of Cambridge Bay (Nunavut, Canada) that bisect Dease Strait in a north-south direction (Fig. 1). These islands create narrow constrictions where localized currents can be much stronger than is typical for the region. Our study builds on work conducted by Dalman et al. (2019), who described an invisible polynya between the islands. Their study found patterns whereby areas with stronger under-ice currents experienced thinner ice (by approximately 20cm, or 10%) and higher bottom-ice algae biomass (about 2-6 times greater Chlorophyll *a* (Chl *a*) biomass). Dalman et al. (2019) concluded that stronger current velocities reduce the ice growth rate by enhancing ocean heat flux to the bottom of the ice, and stimulate ice algal growth through turbulent resupply of nutrients. To study the effect of these conditions on the sea ice carbonate system, we selected two level ice sites (Fig. 1) based on Dalman et al. (2019): one approximately 5 km to the east of the islands, outside of the polynya where we expected weaker currents and thick first-year ice (TFYI, within 100 m of their site 5), and one directly between the islands, in the polynya where we expected strong currents and thin first-year ice (POLY, within 100 m of their site 2).

Sampling was conducted over a 6-day period between 4 and 10 May 2019, with both sites visited on three days (4, 7, and 10 May). On the first sampling date, inverted tilt current meters (Lowell Instruments TCM-1 Current Meter) were installed at both sites, 30 cm below the bottom of the ice. The current meters recorded velocity and temperature for 20 seconds of each minute at a frequency of 16

Hz, which was averaged to 1-minute intervals in post-processing. The instruments were removed on 10
195   May, producing a 6-day record of under ice current velocities.

Sea ice sampling was conducted at the sites using a Kovacs Mark II 9-cm diameter coring system. The
following general considerations were observed for all cores: snow depth was measured with a meter
stick prior to collection; ice thickness was measured after core collection using a Kovacs measuring
tape; when removing cores, the bottoms were pointed away from the sun and shaded to minimize
200   exposure of the ice algal community; and equipment that produced exhaust (snowmobiles, generators)
were positioned downwind of the sampling site. One core was collected at each site on each day for
temperature and salinity profiles. Temperature was measured using a Thermopen Mk4 temperature
probe inserted into holes drilled at 10-cm intervals. The core was cut into 10-cm sections, which were
sealed in plastic bags and transported back to the field lab where they were melted and analyzed for
205   salinity using a YSI multiparameter probe.

For sea ice carbonate sampling we followed the procedure and materials of Hu et al. (2018). After
collecting a core, 10-cm sections were cut in the field, placed into a gas-tight bag, and immediately
vacuum sealed using a commercial meat sealer. The sealed samples were transported back to the field
lab and allowed to melt in the dark at room temperature for 15-20 hours. Meltwater was then transferred
210   to 160-mL borosilicate bottles using a peristaltic pump. The pump was operated at low speed, and water
was pumped from the bottom of the bag to the bottom of the bottle. The sample bottles were triple
rinsed and overflown during filling as per Dickson et al. (2007). Samples were then fixed with 80 µL of
saturated mercuric chloride (0.05% of the total sample volume, as per Dickson et al., (2007)) to prevent

biological activity, and sealed using chlorobutyl-isoprene rubber stoppers and aluminium caps (Jiang et
al., 2008). Samples were stored in the dark until analysis, which occurred within 3 months of collection.

At each site, we obtained one "high-resolution" core for TIC and TA (10 May), where sections were collected every 10 cm from top to bottom. The purpose of the high-resolution core was to qualitatively compare the vertical distribution of TIC and TA between the two sites. But as described in Miller et al. (2015), the inherent heterogeneity of sea ice makes it difficult to quantitatively compare single samples between two sites. To address this, we designed a statistical sampling method where on each date, 5 locations were randomly selected within a 10-m radius of the centre point of each site. At each of these locations a core was extracted, and we collected the top, bottom, and middle 10 cm for TIC and TA analysis. The middle horizon was determined by measuring the length of each core before sectioning, and then collecting a section that spanned the centre of the core. The rest of the core volume was discarded. This yielded a total of 15 samples for each horizon (top, middle, bottom) for each site.

To obtain enough sample volume for a bottom ice Chl a measurement at both sites, the bottom 5 cm of three additional cores were combined ("pooled") in an opaque jug. At each site we collected duplicate samples following this procedure, except on the final sampling day where a single pooled sample was collected at each site. Following Dalman et al. (2019), the cores were melted in the cooler jug with filtered seawater added at a 3:1 ratio to reduce osmotic stress on the algae. The melted samples were filtered onto 25-mm GFF filters in a dark room within 48 hours of collection. The filter papers were then packaged in light-impenetrable foil, frozen, and transported to the University of Manitoba for Chl a analysis.

During our study, we did not collect under-ice seawater samples for carbon system analysis. In past studies, under-ice seawater samples have been used as a reference to compare against sea ice chemistry.

Deleted: ,
Deleted: b
Deleted: chlorophyll-a
Deleted: using
Deleted: unburnt
Deleted: in a dark room
Deleted: lab
Deleted: papers

Instead, we relied on seawater carbonate system measurements we collected in summer from a small
research vessel stationed in Cambridge Bay (see for e.g., Williams et al., 2018). To develop a seawater reference, we averaged all salinity, TA, and TIC samples collected annually below the summer halocline from 2016 to 2019 (n=5) at station R3 (68.97°N, 105.47°W) which is within 15 km of the sampling sites. This yielded a seawater reference (or "endmember") of S_{ref} = 28.8 (±0.4), TA_{ref} = 2058 $\mu mol\ kg^{-1}$ (±42), TIC_{ref} = 1970 $\mu mol\ kg^{-1}$ (±16).

A complimentary survey of snow and ice conditions at the polynya was conducted separately from our primary study by a collaborating research team. On 12 May, 10 sites at 500-m spacing were visited across the northern end of the polynya, approximately 1 km north of POLY (Fig. 1). Snow depth was measured at every site, and ice thickness was measured every second site. We use those results in this paper to examine the spatial extent of the invisible polynya.

2.3 Laboratory methods

Sea ice melt samples were analyzed at the University of Calgary. TIC was determined through acid extraction using an automated sample preparation system (AIRICA by Marianda) that quantifies released CO_2 using an infrared gas analyzer (LiCOR LI-7000). Four TIC replicates of 1.5 mL were analyzed for each sample; the replicate with the highest coefficient of variation was discarded, and the average of the three remaining replicates was calculated. TA was measured by modified Gran Titration (Grasshoff et al., 1999) using a semi-automated open-cell titration system (AS-ALK2 Apollo SciTech) (Cai et al., 2010). Replicates were conducted until two measurements with a coefficient of variation of less than 0.002 were obtained and then averaged. Both instruments were calibrated prior to measurement using certified reference material (CRM batch no 177) from the Scripps Institution of Oceanography of the University of California, San Diego. Precision better than ±1.5 $\mu mol\ kg^{-1}$ was

obtained for TIC, and better than ± 3.2 μmol kg^{-1} for TA. Remaining sample water was then analyzed for salinity using an Orion Star A222 conductivity meter paired with a 013010MD conductivity cell, calibrated daily to a NIST traceable standard.

Chlorophyll a concentration was determined by fluorometry. Frozen filters were placed in scintillation
275   vials with 10 mL of 90% acetone in the dark, briefly agitated on a vortex mixer, and then kept at 4°C for 24 h to extract pigment. Chl a fluorescence was then measured (Turner Designs Trilogy fluorometer) before and after acidifying with 5% HCl following Parsons et al. (1984). From these measurements, the concentration of Chl a was calculated following equations of Holm-Hansen et al. (1965) and a correction for filtered seawater dilution. Concentrations were converted to biomass (e.g. Chl a
280   expressed as mg m^{-2}) by multiplying by the length of the core section collected (in this case, 5 cm or 0.05 m).

2.4 Statistical and remote sensing analysis

Due to the number of samples collected for TIC/TA at the three horizons, and for snow depth and ice
    thickness, we were able to test for statistically significant differences between sites using analysis of
285   variance (ANOVA). ANOVA tests whether the variance between sample groups (i.e., the two sites) is greater than the variance within the sample group (i.e., at a single site). In our application, it tests the null hypothesis that the mean value of any given variable (TIC, TA, snow depth, ice thickness) at the polynya site (POLY) is equal to the mean at the thick ice site (TFYI). A p-value is generated, which communicates the probability of incorrectly rejecting the null hypothesis due to sampling error.
290   ANOVA is a useful method for relatively small sample sizes (in this case, n~15), because it is robust

against modest departures from normally distributed and homoscedastic sample groups (Burt et al., 2009).

The evolution of sea ice cover during freeze-up was reconstructed from high-resolution (6.25 km
295 resolution) AMSR2 imagery. Daily sea ice concentration data from October to November 2018 were obtained from the Universität Bremen open access server (Comiso et al., 2003). The imagery was georeferenced and followed the threshold of 10% sea ice concentration as the boundary between sea ice and open ocean (Spreen et al., 2008).

3 Results

300 ### 3.1 Physical and biological conditions at the sites

The polynya site, POLY, experienced considerably higher under-ice currents, with peak velocities an order of magnitude higher (20 to 40 cm s^{-1} vs. 2 to 4 cm s^{-1}) than outside the polynya, TFYI (Fig. 2 and Table 1). Current velocities at POLY increased throughout the deployment but remained constant at TFYI. The increase in currents at POLY were likely due to a spring tide, but this was difficult to
305 confirm with the Cambridge Bay tidal stage predictions (Fig. S1) where amplitudes are low due to the wide geometry of the bay.

Snow and ice conditions also appeared to be different at the two sites (Table 1) with the mean ice thickness at TFYI about 33 cm (20%) thicker than at POLY. Conversely, the polynya site experienced deeper snow, by an average of 11 cm or about 40%. Ice temperature profiles (Fig. 3) show that on the
310 first two sampling days (4, 7 May) the ice in the polynya was warmer than the thick FYI, by about 2°C

315 at most depths. The temperature at both sites increased on the final sampling day – by 2 to 3°C at the surface and 1 to 1.5°C in the middle of the ice – relative to the first sampling day. This observation is consistent with air temperatures recorded at the Environment Canada weather station in Cambridge Bay, which showed daytime highs increasing from -13°C to -3°C, and nighttime lows increasing from - 22°C to -13°C (Fig. S2) during the study period. Ice surface temperatures remained below -6°C on all

320 dates (Fig. 2), and we made no visual observations of melt onset in the snowpack.

In contrast to the results of Dalman et al. (2019), bottom ice algal biomass was about 3 times higher at TFYI than at POLY (Table 1). Although we did not collect nearly as many ices algal samples compared to other variables, the range and standard deviations reported in Table 1 show consistency between dates. These results match well with our field observations of much higher visible ice algae at TFYI site

325 on essentially all the cores we extracted.

3.2 Carbonate chemistry at the Sites

Results from the high-resolution cores collected on 10 May are shown in Fig. 4. The polynya site was characterized by "c-shaped" profiles for TIC, TA, and salinity, with relatively higher values at the top and bottom of the core compared to the middle. The TFYI site did not have elevated values at the top of

330 the ice but did display an increase in all parameters in the lowest horizon. The profiles show divergence between sites in the upper and lower ice horizons, but consistency throughout most of the ice volume.

The results from the statistical sampling approach are shown in Tables 2 and 3, and confirm the general patterns observed in Fig. 4. In the upper ice horizon TIC, TA, and salinity was significantly higher (by 62, 70, and 1.3 µmol kg^{-1}, respectively) at POLY compared to TFYI. The middle horizon was

335 statistically indistinguishable between the two sites for all three parameters. In the bottom ice horizon,

the POLY site experienced significantly lower TIC, TA, and salinity (by 87, 73, and 1.1 μmol kg^{-1}, respectively) than the TFYI site. TA:TIC ratios are also displayed in Tables 2 and 3. These ratios were

340 not statistically different in the top or middle ice horizons but were significantly different in the bottom horizon.

4 Discussion

4.1 Physical and biological differences between sites

Table 3 shows that the polynya site had statistically thinner ice and thicker snow than the non-polynya

345 site. The strong currents we observed are consistent with a polynya formation mechanism related to enhanced ocean heat flux, as detailed in Melling et al. (2015). Melling et al. (2015) also hypothesized deep snow as a potential cause of invisible polynyas but noted that variations in snow depth usually occur over scales too large (i.e., hundreds of km) or too small (snow drifts) to be considered polynyas. For our dataset, we cannot rule out snow depth as a contributing factor to the invisible polynya;

350 however, Dalman et al. (2019) demonstrated ice thickness was significantly different between sites when snow depth was controlled for during site selection. Sea ice thermodynamic models (e.g., Flato and Brown, 1996) predict that maximum ice thickness should vary by about 10% for the difference in snow accumulation that was observed at the two sites. Such differences are supported by observational studies (e.g., Howell et al. 2016). In our study, the 33cm (20%) thinner ice at the polynya site is

355 probably too great to be explained by snow depth alone, but it is not unreasonable to estimate that snow may have been responsible for about half of the difference.

Of course, snow depth is spatially variable over many scales and the differences we observed between the two sites could have been due to small scale drifting. However, the long transect conducted on 12

May (Fig. 5) shows a consistent pattern of deeper snow and thin ice in the vicinity of the island to the north (Fig. 1). Local knowledge shared with us by guides is that prevailing winds in this area are from the northeast. It is possible that large-scale drifts form on the downwind side of the island (Fig. 1), contributing to the thinner ice. The timing of ice consolidation is also important, as ice that forms earlier

365   in the season has longer to accumulate snow. Maps of sea ice concentration that we acquired for the freeze-up season show that ice at the two sites consolidated at roughly the same time (Fig. 6).

The distribution of ice algal biomass we observed was different from that reported in Dalman et al. (2019) who reported Chl a biomass averaging 9.3 mg m^{-2} at the polynya site and 1.4 mg m^{-2} at the thick ice site (c.f. Table 2) with an average snow thickness of 2.8 +/- 0.5 cm. Not only did we observe higher

370   bottom ice Chl a at TFYI relative to POLY, but we also observed higher average biomass there than at any of the sites reported in Dalman et al. (2019). Snow depth is the dominant limiting factor influencing local ice algal distribution in the Arctic during early spring (e.g., Welch and Bergmann, 1989; Mundy et al., 2005; Campbell et al., 2015; Lange et al. 2019), with snow depths > 25 cm limiting ice algal accumulation well into the spring season (Leu et al. 2015). Therefore, it is most likely that light

375   limitation under thick snow at the polynya site overshadowed any potential boost in production from current-driven nutrient supply. It is unclear why Dalman et al. (2019) observed lower Chl a biomass under a thinner snow cover in a previous year. Photoacclimation (e.g., Campbell et al., 2015) is one possibility, but with limited data it is difficult to know what the role of interannual variability is on ice algae biomass.

380   **4.2 The upper-ice horizon**

Significantly higher salinity in the top 10 cm at the polynya site compared to the thick FYI (Table 3) is likely a result of initial ice formation conditions. Typically, higher salinity is associated with faster ice

growth rates (Cox and Weeks, 1974). Sea ice in this region began to form around 15 October and did

not fully consolidate until 7 November. (Fig. 6). Due to the redistribution of drifting ice early in the fall,

390   it is possible the ice that eventually consolidated in the polynya region did experience a different

(potentially faster) initial growth rate. However, another explanation is that ice formation at the two

sites occurred under different turbulence conditions, with the polynya site experiencing greater

turbulence due to strong tidal currents. As reviewed in Weeks (2010), turbulent ice formation conditions

promote frazil ice production, while calm conditions favour congelation growth. In an extensive

395   analysis of sea ice texture in the Canadian Arctic, Carnat et al. (2013) found the depth of surface frazil

to vary between 0 – 15 cm due to different turbulence regimes. It is possible that the frazil ice layer was

thicker at POLY than TFYI, although confirmation would have required thin section analysis. The

randomly oriented nature of frazil crystals could act to trap more salts and thus yield higher bulk salinity

(as we observed at POLY), but this has not been extensively studied. In a study of Antarctic ice, Eicken

400   (1992) did observe slightly higher salinities in ice cores characterized by frazil ice, but not high enough

to be considered statistically significant. Another potential cause of differences at the surface between

sites is flooding, the process that occurs when relatively thick snow covers depress the ice surface below

the freeboard level, allowing seawater to flow over the ice. Flooding is less common in the Arctic than

the Antarctic due to relatively thinner snowpacks and thicker ice (Provost et al., 2017), and during our

405   study period we observed positive freeboard at all sites. But given the deeper snowpack at POLY, it is

possible that flooding occurred earlier in the season when the ice was still quite thin. As described by

Eicken et al. (1992), this would lead to higher surface salinity.

The standard deviation of salinity may be a better indication of ice formation conditions; Weeks and

Lee (1962) found the standard deviation of salinity in pancake ice to be greater than 1.0, while

410   congelation ice had a standard deviation greater than 0.3 – 0.5. Table 2 shows the standard deviation of

salinity we observed was indeed much higher at the polynya site (1.2) than the thick first year ice site

(0.4). Pancake ice typically forms under significant ocean swell, which we would not expect in these

narrow coastal passages. However, the general concept that turbulent growth conditions lead to higher

415 variability holds for frazil ice (Weeks, 2010) and provides support for the interpretation that salinity

variations between sites in the upper ice horizon was caused by different turbulence regimes. Weeks and Lee (1962) also noted that brine drained much more slowly from pancake ice, which could explain the higher salinity we observed at the polynya site.

At first glance, the statistically higher TIC and TA in surface ice at the polynya site (Table 3) appear to

420 be explainable in the context of bulk salinity and brine rejection. Salinity is a conservative tracer of brine rejection, and if sea ice carbonate chemistry were only impacted by brine rejection, we would expect bulk TIC and TA to be higher when bulk salinity is higher. Hence the observations between the two sites make sense, and the preceding discussion about processes controlling salinity apply to the carbonate system as well: TIC and TA were probably higher in the surface at the polynya due to ice

425 formation under different turbulence conditions.

However, more nuances become apparent in Fig. 7, which compares the sea ice carbonate system and salinity measurements to a mixing line between a pure ice endmember (salinity, TIC, TA = 0) and our reference seawater endmember (see section 2.2). Figure 7 shows that while the bottom and middle samples collected at both sites follow the mixing line, the top core sections are substantially lower (for

430 both TIC and TA) than the mixing line. The average differences (Δ) between the core samples in the top horizon and the mixing line were ΔTIC = -118 μmol kg^{-1}, ΔTA = -78 μmol kg^{-1} at POLY, and ΔTIC = -87 μmol kg^{-1}, ΔTA = -52 μmol kg^{-1} at TFYI. This indicates a process (or processes) other than brine rejection that affected TA and TIC at the top of the ice.

Calcium carbonate (i.e., ikaite) precipitation lowers both TIC and TA, which can help explain the

435 observed depletions in the surface ice. However, precipitation alone would result in TA being twice as

depleted as TIC, and what we observed is the opposite (TIC was depleted at about twice the rate of TA). Gas evasion is a strong candidate for explaining large depletions in TIC and is consistent with past measurements of CO_2 offgassing by sea ice (e.g., Nomura et al., 2006; 2010), and observations of TIC loss in the surface layer of bulk ice samples (Miller 2011a). The larger reduction in TIC at the polynya site suggests that ice texture (e.g., frazil vs. congelation ice) may have an impact on CO_2 release potential, but to our knowledge this has not been investigated in any detail in past studies. It is still possible that ikaite formation occurred in these upper layers and is the most logical explanation for depleted TA relative to the mixing line. For ikaite production to cause a depletion in bulk sea ice TA the crystals must not have been retained in the ice matrix, instead transported to lower ice horizons or the underlying ocean during the rapid brine drainage that occurs in new ice (Vancoppenolle et al. 2006).

4.3 The middle-ice horizon

Observations and modeling studies have emphasized a strong relationship between ice growth rate and bulk salinity (e.g., Cox and Week, 1975; Vancoppenolle et al., 2006). Rapidly growing ice tends to trap more brine, resulting in higher bulk salinity. We therefore anticipated lower salinity and perhaps lower TA and TIC in the polynya ice where enhanced ocean heat flux (and thicker snow cover) reduced the ice growth rate. Furthermore, Feltham et al. (2002) proposed that strong under ice currents might enhance brine drainage by inducing pressure variations at the ocean-ice interface, in which case salinity at the polynya site might be even lower. Table 3 shows that our expectations were not met, with no statistical difference in salinity, TA, or TIC observed in the middle horizons. Figure 7 shows that the carbonate species closely followed the conservative mixing line in the middle ice horizon, and that salinity at both sites fell within a well-defined band of approximately 4 – 5.5. Due to the strength of this

440

445

450

455

Deleted: Nomura, Nomura

Deleted: studied

Deleted: salt

Deleted: DIC

salinity relationships, and the similar salinity between sites, we did not observe a significant difference in carbonate system parameters.

Salinity (and hence TA and TIC) may have been similar because the growth rates are not so
465 dramatically different between sites for this portion of the ice volume. Much of the observational and modeling work relating salinity to ice growth rates has focused on resolving the C-shaped profile of sea ice (e.g., Fig. 4c), which reflects high brine retention during fast initial ice growth (creating higher salinity in the top horizon than the middle horizon), followed by brine drainage (creating lower salinity in the middle horizons compared to the bottom horizon). Under typical Arctic conditions, the top 20 cm
470 of sea ice can grow in approximately 15 days, for a growth rate of 1.3 cm day^{-1} (e.g., Nakawo and Sinha, 1981). If we assume sea ice formed in the study area around 15 October (Fig. 6), and the first 20 cm grew by 30 October, that would imply an average "middle horizon" growth rate of about 0.6 cm/day for the polynya site and 0.7 cm/day for the thick FYI site from the end of October to the sampling date. We hypothesize that large differences in initial growth rates compared to later winter growth rates are
475 enough to produce significant vertical variations in salinity, but the small differences in growth rates between the two sites was not enough to produce noticeable differences in salinity, nor in TIC or TA.

4.4 The bottom-ice horizon

Past studies have shown low TIC in the bottom sections of bulk ice melts (Brown et al., 2015) and in brine collected from lower ice horizons (Brown et al., 2015, Delille et al., 2007) in spring sea ice. These
480 lower values are typically attributed to biological drawdown caused by the bottom-ice algal bloom. In our results, we saw significantly higher TIC and TA (Table 3) at the site with higher Chl a (TFYI, Table 1). This counterintuitive result is explained again by salinity: TFYI had significantly higher salinity than POLY at the bottom (Tables 2, 3), and Figure 7 shows that the bottom ice horizons largely followed the

conservative mixing line. It is interesting to note that lower salinity at the site with high current velocity
follows the Feltham et al. (2002) prediction that strong under-ice currents drive easier replacement of
high-salinity brine with (relatively) lower salinity seawater. But as noted previously, this is not reflected
in the middle ice horizon. Notz and Worster (2009) found that the majority of salt is lost from sea ice
through gravity drainage, not at the growing front. Once out of direct contact with the seawater,
variables other than current velocity (e.g., thickness, temperature gradient, and brine salinity) may
determine salinity (Notz and Worster, 2009). If these factors are relatively consistent between sites, we
would expect salinity (and hence TIC and TA) to also be similar. Nevertheless, it is clear that physical
processes (brine rejection) and not biological processes (i.e., the ice algae bloom) were most responsible
for carbonate system differences between the two sites in the bottom layer.

To further check for the impact of primary production on the bottom ice horizon (and any of the other
horizons) we normalized TIC and TA values to the estimated seawater endmember salinity (S_{ref} = 29)
using $nX = \frac{X_{meas}}{S_{meas}} \times S_{ref}$, where nX is the normalized parameter (TIC or TA), X_{meas} is the bulk ice
measurement, and S_{meas} is the measured bulk salinity. This is the appropriate normalization equation for
a system where the $S = 0$ endmember is expected to have a TA and TIC equal to 0 µmol kg^{-1} (Friis et
al., 2003), which is the case for pure ice. If primary production were significantly affecting any of the
ice horizons, we would expect points on a graph of nTA vs. nTIC (Fig. 8) to fall along the
photosynthesis/respiration line. Although statistically significant linear trends (p < 0.01) are apparent at
both sites, and in all horizons, they do not follow the photosynthesis line, even in the bottom ice horizon
(Table 4). The slopes that we observed of nTA vs. nTIC all fell within the range of 0.50 – 1.03, with an
overall slope of 0.65 at TFYI and 0.81 at POLY (Fig. 8). In their study of landfast sea ice in the

505 Canadian Arctic Archipelago (Franklin Bay), Miller et al. (2011a) did see a few samples from May that
fell along a photosynthesis line, but most followed a very similar slope to the ones presented in Fig. 8.

It may however be more instructive to consider the slope of the bottom horizon alone (Table 4), as the
overall slopes are biased by the high number of samples collected at the surface and bottom, despite
representing only a small portion of the overall ice volume. In the bottom horizon, we do see lower
510 slope values (0.67 at TFYI, 0.50 at POLY), suggesting a shift towards the net respiration line, consistent
with past studies that have found net heterotrophy in ice algae communities during the bloom (Campbell
et al., 2017,2022; Rysgaard and Glud, 2004). In the 2014 spring, Campbell et al. (2017) observed net
heterotrophic conditions in the bottom ice of Dease Strait during a period of carbon accumulation,
before switching to autotrophic conditions around 8-May. In a study near Resolute Bay, Brown et al.
515 (2015) found substantial TIC drawdown near the beginning of an ice algae bloom, but that region
experiences bottom ice Chl *a* value about 10 times higher than either of our sites (Leu et al., 2015). It is
possible that the rate of ice algal production in Dease Strait is simply too low to have a noticeable
impact on carbonate chemistry, or that primary production at our site was balanced or exceeded by
respiration, highlighting that sea ice algae communities may have a complex role in carbon cycling in
520 sea ice.

4.5 Implications for understanding ikaite in sea ice

The carbonate chemistry of sea ice has garnered significant attention due to questions surrounding ikaite
precipitation and dissolution. Our preceding analysis of the three ice horizons only invoked ikaite

precipitation to explain patterns observed in the top horizon, where it seemed a secondary process to gas exchange. So, is ikaite precipitation apparent (or important) in our samples?

The primary evidence presented by Rysgaard et al. (2007) and Rysgaard et al. (2009) to support the hypothesis of ikaite precipitation was the observation of TA:TIC ratios greater than 1:1 and approaching
530 2:1 in some samples. The only relatively high TA:TIC ratios that we observed were in the upper ice horizon (Table 2), which other studies (Miller et al. 2011a; Geilfus et al. 2013) have observed and attributed primarily to outgassing from the ice surface. But average TA:TIC ratios in our samples were close to 1.05 in the bottom and middle ice horizons (Table 1), and not meaningfully different from our estimate of the source seawater TA:TIC ratio (1.04). While the original formulation of the sea ice pump
535 hypothesis (Rysgaard et al., 2007) reported bulk TA:TIC ratios approaching 2:1, the majority of studies since have reported values close to 1:1 below the surface ice layers (Miller et al., 2011a, 2011b; Geilfus et al., 2012; Brown et al., 2015; Findlay et al., 2015).

Of course, the TA:TIC ratio is not the only available evidence of ikaite precipitation in sea ice. There is microscopic evidence (e.g., Rysgaard et al., 2013), and crystals extracted from sea ice have been
540 positively identified by x-ray diffraction (Dieckmann, et al. 2008). We did not have access to such techniques, but Figure 8 provides evidence that ikaite precipitation did occur in our study. At both sites, linear relationships between nTIC and nTA with slopes between 0.5 and 1.0 (Table 4), were observed through all horizons. These slopes are similar to those observed by Miller et al. (2011a), who hypothesized that such a relationship is the result of combined ikaite precipitation and respiration in the
545 ice. Similar slope values were observed by Geilfus et al. (2012) and Brown et al. (2015) in brine. The differences we observed in slopes between horizons are likely the result of specific processes occurring near the surface (i.e. outgassing, see section 4.2) and the bottom (net respiration, see section 4.4) but with a strong tendency towards the carbonate precipitation/dissolution line in all horizons. Therefore,

ikaite precipitation certainly seems to be occurring in our study area; our contention is simply that at this location (and apparently at several others) the amount of ikaite precipitation is not enough to result in a large fractionation of TA and TIC within the sea ice. Or perhaps more precisely, ikaite crystals are lost to the underlying seawater at a similar rate to brine rejection.

560 The well-known spatial heterogeneity of sea ice has often been invoked to explain differences between studies, including differences in the TA:TIC ratio (compare for example, Rysgaard et al., 2007 and Miller et al., 2011a). Due to the scale of brine channels and the size of the standard core barrel, it is not uncommon for two ice cores sampled essentially side-by-side to produce remarkably different results for any biogeochemical variable (Miller et al., 2015). To our knowledge, the present study is the first

565 attempt to employ a statistical sampling approach to compare sea ice carbonate chemistry between two sites. What our results show is that despite large differences in the physical and biological characteristics between two locations, when small-scale heterogeneity is accounted for by averaging the results can be surprisingly similar. Table 5 shows that when a weighted vertical average of the two sites is calculated, the carbonate chemistry (particularly the TA:TIC ratio) is not meaningfully different; the

570 statistically significant differences in the thin top and bottom layers are outweighed by the thick middle layer. Our study, designed to examine extremes in spatial variability, suggest that we should perhaps be looking at other factors (perhaps methodologies) to explain divergent reports of sea ice carbonate chemistry.

Setting aside the TA:TIC ratio, the actual values of bulk ice TIC and TA (Table 5) that we observed are

575 fairly consistent with other measurements from the Canadian Arctic Archipelago. Rysgaard et al. (2009), Miller et al. (2011a), Findlay et al. (2015) and Brown et al. (2015) all report values between ~300-400 μmol kg^{-1} for TA, and 350-450 μmol kg^{-1} for TIC. Higher values (up to ~700 μmol kg^{-1} for both TIC and TA) have been reported in deep Arctic basins and around Greenland (Rysgaard et al.,

2009). Salinity, and hence carbonate species concentrations, tend to be lower in the Canadian Arctic Archipelago due to the large volume of river runoff that impacts the region. It is therefore likely that the source water from which sea ice grows plays a significant role in winter sea ice carbonate

585   concentrations.

5 Conclusions

We contrasted the bulk sea ice carbonate chemistry of an invisible polynya site (strong currents, thin ice, thick snow, lower algal chl-*a*) with a nearby site outside of the polynya (weak currents, thick ice, thin snow, higher algal chl-*a*). Statistically significant differences in chemistry were noted between the

590   two locations, but only in thin surface and bottom layers. The middle ice horizons – which represent about 85% of the ice volume – had statistically indistinguishable salinity, TIC, and TA concentrations. The observation that two sites with such different physical and biological characteristics could yield such similar carbonate system chemistries suggests that processes known to modify the sea ice carbonate system are either less impactful, or less variable, than expected. While our results do show

595   evidence of some combination of gas evasion, respiration, and ikaite precipitation impacting chemistry, these processes were dominated by brine drainage processes as evidenced by strong relationships with salinity. Although considerable regional variability in bulk ice TIC and TA concentrations are evident when comparing our results to other studies, strong salinity relationships are a consistent result. Therefore, it may be possible to derive an empirical relationship between sea ice salinity and the source

600   seawater chemistry to predict sea ice carbonate chemistry; an outcome which may have utility in modeling studies. It is important to note, however, that the geographical areas currently represented in the literature are fairly limited in scope. We expect regional variability to play an important role; for example the differences we measured in ice algae biomass are considerably lower that the difference between our sites and somewhere like Resolute Bay. An ongoing effort by the Biogeochemical

605   Exchange Processes at Sea Ice Interfaces (BEPSII) working group to compile published and
      unpublished data may reveal complexities that we cannot capture in a single Arctic region. Such an
      effort may also shed light on the important (and unresolved) question of how best to characterize the
      TA:TIC ratio in sea ice.

Acknowledgements

Thanks to Shawn Marriott, Zoe Walker, and the staff of the Canadian High Arctic Research Station who assisted with fieldwork. Alexandre Langois provided the long snow depth/sea ice thickness transect data. We acknowledge the ongoing logistical support of Polar Knowledge Canada and the Arctic Research Foundation. Financial support was provided by the Marine Environmental Observation Prediction and Response (MEOPAR) Network of Centres of Excellence, the ArcticNet Network of Centres of Excellence, the Canada Foundation for Innovation John R. Evans Leaders Fund, the Natural Sciences and Engineering Research Council of Canada (NSERC), and the University of Calgary. A. Cranch was supported by a scholarship from the Northern Science Training Program (NSTP). This paper is a contribution to the SCOR Working Group 152 – Measuring Essential Climate Variables in Sea Ice (ECV-Ice), and the Biogeochemical Exchange Processes at Sea Ice Interfaces network. Thank you to Sébastien Moreau and Eric Mortenson for reviewing this paper, and providing valuable suggestions.

Data Availability

The data used in this manuscript have been made publicly available on the Polar Data Catalogue (https://www.polardata.ca/). Search for CCIN reference number 13263.

References

Back, D.-Y., Ha, S.-Y., Else, B., Hanson, M., Jones, S. F., Shin, K.-H., Tatarek, A., Wiktor, J. M., Cicek, N., Alam, S., and Mundy, C. J.: On the impact of wastewater effluent on phytoplankton in the Arctic coastal zone: A case study in the Kitikmeot Sea of the Canadian Arctic, Science of The Total Environment, 759, https://doi.org/10.1016/j.scitotenv.2020.143861, 2021.

Bates, N. R., and Mathis, J. T.: The Arctic Ocean marine carbon cycle: evaluation of air-sea CO_2 exchanges, ocean acidification impacts and potential feedbacks, Biogeosciences, 6, 2433–2459, https://doi.org/10.5194/bg-6-2433-2009, 2009.

Brown, K. A., Miller, L. A., Mundy, C. J., Papakyriakou, T., Francois, R., Gosselin, M., Carnat, G., Swystun, K., and Tortell, P. D.: Inorganic carbon system dynamics in landfast Arctic Sea ice during the early-melt period, J. Geophys. Res. Oceans, 120, 3542–3566, https://doi.org/10.1002/2014JC010620, 2015.

Burt, J. E., Barber, G. M., and Rigby, D. L.: Elementary Statistics for Geographers, Third Edition, 3rd edition., The Guilford Press, New York, 653, 2009.

Cai, W.-J., Hu, X., Huang, W.-J., Jiang, L.-Q., Wang, Y., Peng, T.-H., and Zhang, X.: Alkalinity distribution in the western North Atlantic Ocean margins, J. Geophys. Res., 115, https://doi.org/10.1029/2009JC005482, 2010.

Campbell, K., Mundy, C. J., Barber, D. G., and Gosselin, M.: Remote Estimates of Ice Algae Biomass and Their Response to Environmental Conditions during Spring Melt, Arctic, 67, 375-387-375–387, https://doi.org/10.14430/arctic4409, 2014.

Campbell, K., Mundy, C. J., Barber, D. G., and Gosselin, M.: Characterizing the sea ice algae chlorophyll a–snow depth relationship over Arctic spring melt using transmitted irradiance, Journal of Marine Systems, 147, 76–84, https://doi.org/10.1016/j.jmarsys.2014.01.008, 2015.

Campbell, K., Mundy, C. J., Landy, J. C., Delaforge, A., Michel, C., and Rysgaard, S.: Community dynamics of bottom-ice algae in Dease Strait of the Canadian Arctic, Progress in Oceanography, 149, 27–39, https://doi.org/10.1016/j.pocean.2016.10.005, 2016.

Campbell, K., Mundy, C. J., Gosselin, M., Landy, J. C., Delaforge, A., and Rysgaard, S., Net community production in the bottom of first-year sea ice over the Arctic spring bloom, *Geophysical Research Letters*, *44*(17), 8971–8978, https://doi.org/10.1002/2017GL074602, 2017.

Campbell, K., Lange, B.A., Landy, J.C., Katlein, C., Nicolaus, M., Anhaus, P, Matero, I., Gradinger, R., Charette, J., Duerksen, S., Tremblay, P, Rysgaard, S., Tranter, M., Haas, C., Michel, C., Net heterotrophy in High Arctic first-year and multi-year spring sea ice, Elementa: Science of

665   the Anthropocene 4 January 2022, 10 (1): 00040, https://doi.org/10.1525/elementa.2021.00040, 2022.

Carnat, G., Papakyriakou, T., Geilfus, N., Brabant, F., Delille, B., Vancoppenolle, M., Gilson, G., Zhou, J., and Tison, J.: Investigations on physical and textural properties of Arctic first-year sea ice in the Amundsen Gulf, Canada, November 2007–June 2008 (IPY-CFL system study), J. Glaciol., https://doi.org/10.3189/2013JoG12J148, 2013.

Chalmers, B. and Williamson, R. B.: Crystal Multiplication without Nucleation, Science, 148, 1717–1718, https://doi.org/10.1126/science.148.3678.1717, 1965.

Comiso, J. C., Cavalieri, D. J., and Markus, T.: Sea ice concentration, ice temperature and snow depth using AMSR-E data. IEEE Geoscience and Remote Sensing Letters, 41(2), 243–252, https://doi.org/10.1109/TGRS.2002.808317, 2003.

Cox, G. F. N. and Weeks, W. F.: Salinity Variations in Sea Ice, J. Glaciol., 13, 109–120, https://doi.org/10.3189/S0022143000023418, 1974.

Cox, G. F. N., and Weeks, W. F.: Brine drainage and initial salt entrapment in sodium chloride ice, CRREL Res. Rep. 345, U.S. Army Cold Reg. Res. and Eng. Lab., Hanover, N. H, 1975.

Dalman, L. A., Else, B. G. T., Barber, D., Carmack, E., Williams, W. J., Campbell, K., Duke, P. J., Kirillov, S., and Mundy, C. J.: Enhanced bottom-ice algal biomass across a tidal strait in the Kitikmeot Sea of the Canadian Arctic, Elementa: Science of the Anthropocene, 7, https://doi.org/10.1525/elementa.361, 2019.

Delille, B., Jourdain, B., Borges, A. V., Tison, J.-L., and Delille, D.: Biogas (CO_2, O_2, dimethylsulfide) dynamics in Spring Antarctic fast ice, Limnol. Oceanogr., 52, 1367–1379, https://doi.org/10.4319/lo.2007.52.4.1367, 2007.

Dickson, A. G., Sabine, C. L., and Christian, J. R. (eds): Guide to Best Practices for Ocean CO_2 Measurements, Sidney, British Columbia, North Pacific Marine Science Organization, PICES Special Publication, 3, 191, https://doi.org/10.25607/OBP-1342, 2007.

Dieckmann, G. S., Nehrke, G., Papadimitriou, S., Göttlicher, J., Steininger, R., Kennedy, H., Wolf-Gladrow, D., and Thomas, D. N.: Calcium carbonate as ikaite crystals in Antarctic Sea ice, Geophys. Res. Lett., 35, L08501, https://doi.org/10.1029/2008GL033540, 2008.

Dieckmann, G. S., Nehrke, G., Uhlig, C., Göttlicher, J., Gerland, S., Granskog, M. A., and Thomas, D. N.: Brief Communication: Ikaite ($CaCO_3.6H_2O$) discovered in Arctic Sea ice, The Cryosphere, 4, 227–230, https://doi.org/10.5194/tc-4-227-2010, 2010.

Eicken, H.: Salinity profiles of Antarctic Sea ice: Field data and model results, J. Geophys. Res., 97, 15545–15557, https://doi.org/10.1029/92JC01588, 1992.

Feltham, D. L., Worster, M. G., and Wettlaufer, J. S.: The influence of ocean flow on newly forming sea ice, J. Geophys. Res., 107, 1-1-1–9, https://doi.org/10.1029/2000JC000559, 2002.

700   Flato, G. M. and Brown, R. D.: Variability and climate sensitivity of landfast Arctic Sea ice, J. Geophys. Res. Oceans, 101, 25767–25777, https://doi.org/10.1029/96JC02431, 1996.

Findlay, H. S., Edwards, L. A., Lewis, C. N., Cooper, G. A., Clement, R., Hardman-Mountford, N., Vagle, S., and Miller, L. A.: Late winter biogeochemical conditions under sea ice in the Canadian High Arctic, Polar Research, 34, 1, https://doi.org/10.3402/polar.v34.24170, 2015.

705   Friis, K., Körtzinger, A., and Wallace, D. W. R.: The salinity normalization of marine inorganic carbon chemistry data, Geophys. Res. Lett., 30, https://doi.org/10.1029/2002GL015898, 2003.

Galley, R. J., Else, B. G. T., Howell, S. E. L., Lukovich, J. V., and Barber, D. G.: Landfast Sea Ice Conditions in the Canadian Arctic: 1983-2009, Arctic, 65, 133–144, https://www.jstor.org/stable/41638586, 2012.

710   Geilfus, N.-X., Carnat, G., Papakyriakou, T., Tison, J.-L., Else, B., Thomas, H., Shadwick, E., and Delille, B.: Dynamics of pCO_2 and related air-ice CO_2 fluxes in the Arctic coastal zone (Amundsen Gulf, Beaufort Sea), J. Geophys. Res., 117, C00G10, https://doi.org/10.1029/2011JC007118, 2012.

Geilfus, N.-X., Galley, R. J., Cooper, M., Halden, N., Hare, A., Wang, F., Søgaard, D. H., and
715   Rysgaard, S.: Gypsum crystals observed in experimental and natural sea ice, Geophys. Res. Lett., 40, 6362–6367, https://doi.org/10.1002/2013GL058479, 2013.

Grasshoff, K., Kremling, K., and Ehrhardt, M.: Methods of Seawater Analysis. 3rd edition. Weinheim: Wiley-VCH., 632, 1999.

Grimm, R., Notz, D., Glud, R. N., Rysgaard, S., and Six, K. D.: Assessment of the sea-ice carbon
720   pump: Insights from a three-dimensional ocean-sea-ice-biogeochemical model (MPIOM/HAMOCC), Elementa: Science of the Anthropocene, 4, https://doi.org/10.12952/journal.elementa.000136, 2016.

Holm-Hansen, O., Lorenzen, J., Holmes, R. W., and Strickland, J. D.: Fluorometric determination of chlorophyll, ICES J. Mar. Sci., 30(1), 3–15, https://doi.org/10.1093/icesjms/30.1.3, 1965.

725   Howell, S. E. L., Laliberté, F., Kwok, R., Derksen, C., and King, J.: Landfast ice thickness in the Canadian Arctic Archipelago from observations and models, The Cryosphere, 10, 1463–1475, https://doi.org/10.5194/tc-10-1463-2016, 2016.

Hu, Y., Wang, F., Boone, W., Barber, D., and Rysgaard, S..: Assessment and improvement of the sea ice processing for dissolved inorganic carbon analysis, Limnol. Oceanogr.-Meth., 16, 83-91,
730   https://aslopubs.onlinelibrary.wiley.com/doi/full/10.1002/lom3.10229, 2018.

Jiang, L.-Q., Cai, W.-J., and Wang, Y.: A comparative study of carbon dioxide degassing in river- and marine-dominated estuaries, Limnol. Oceanogr., 53, 2603–2615, https://doi.org/10.4319/lo.2008.53.6.2603, 2008.

König, D., Miller, L. A., Simpson, K. G., and Vagle, S.: Carbon Dynamics During the Formation of Sea Ice at Different Growth Rates, Front. Earth Sci., 6, https://doi.org/10.3389/feart.2018.00234, 2018.

Lange, B. A., Haas, C., Charette, J., Katlein, C., Campbell, K., Duerksen, S., Coupel, P., Anhaus, P., Jutila, A., Tremblay, P. O. G., Carlyle, C. G., and Michel, C.: Contrasting Ice Algae and Snow-Dependent Irradiance Relationships Between First-Year and Multiyear Sea Ice, Geophys. Res. Lett., 46, 10834–10843, https://doi.org/10.1029/2019GL082873, 2019.

Leu, E., Mundy, C. J., Assmy, P., Campbell, K., Gabrielsen, T. M., Gosselin, M., Juul-Pedersen, T., and Gradinger, R.: Arctic spring awakening – Steering principles behind the phenology of vernal ice algal blooms, Progress in Oceanography, 139, 151–170, https://doi.org/10.1016/j.pocean.2015.07.012, 2015.

Manizza, M., Menemenlis, D., Zhang, H., and Miller, C. E.: Modeling the Recent Changes in the Arctic Ocean CO_2 Sink (2006–2013), Global Biogeochemical Cycles, 33, 420–438, https://doi.org/10.1029/2018GB006070, 2019.

Martin, S. and Kauffman, P.: A Field and Laboratory Study of Wave Damping by Grease Ice, J. Glaciol., 27, 283–313, https://doi.org/10.3189/S0022143000015392, 1981.

Melling, H., Haas, C., and Brossier, E.: Invisible polynyas: Modulation of fast ice thickness by ocean heat flux on the Canadian polar shelf, J. Geophys. Res. Oceans, 120, 777–795, https://doi.org/10.1002/2014JC010404, 2015.

Meiners, K. M., Vancoppenolle, M., Thanassekos, S., Dieckmann, G. S., Thomas, D. N., Tison J.-L., Arrigo, K. R., Garrison, D. L., McMinn, A., Lannuzel, D.,van der Merwe, P., Swadling, K. W., Smith Jr., W. O., Melnikov, I., and Raymond, B.: Chlorophyll a in Antarctic sea ice from historical ice core data, Geophys. Res. Lett., 39, L21602, https://doi:10.1029/2012gl053478, 2012.

Meiners, K. M., Vancoppenolle, M., Carnat, G., Castellani, G., Delille, B., Delille, D., Dieckmann, G. S., Flores, H., Fripiat, F., Grotti, M., Lange, B. A., Lannuzel, D., Martin, A., McMinn, A., Nomura, D., Peeken, I., Rivaro, P., Ryan, K. G., Stefels, J., Swadling, K. M., Thomas, D. N., Tison, J.-L., van der Merwe, P., van Leeuwe, M. A., Weldrick, C., and Yang, E. J.: Chlorophyll-a in Antarctic landfast sea ice: A first synthesis of historical ice core data, J. Geophys. Res. Oceans, 123, 8444–8459, https://doi.org/10.1029/2018JC014245, 2018.

765 Miller, L., Papakyriakou, T., Collins, R., Deming, J., Ehn, J., Macdonald, R., Mucci, A., Owens, O., Raudsepp, M., and Sutherland, N.: Carbon dynamics in Sea Ice: A Winter Flux Time Series, Journal of Geophysical Research, 116, C02028, https://doi.org/10.1029/2009JC006058, 2011a.

Miller, L. A., Carnat, G., Else, B. G. T., Sutherland, N., and Papakyriakou, T. N.: Carbonate system evolution at the Arctic Ocean surface during autumn freeze-up, J. Geophys. Res., 116, https://doi.org/10.1029/2011JC007143, 2011b.

770 Miller, L. A., Fripiat, F., Else, B. G. T., Bowman, J. S., Brown, K. A., Collins, R. E., Ewert, M., Fransson, A., Gosselin, M., Lannuzel, D., Meiners, K. M., Michel, C., Nishioka, J., Nomura, D., Papadimitriou, S., Russell, L. M., Sørensen, L. L., Thomas, D. N., Tison, J.-L., van Leeuwe, M. A., Vancoppenolle, M., Wolff, E. W., and Zhou, J.: Methods for biogeochemical studies of sea ice: The state of the art, caveats, and recommendations, Elementa: Science of the 775 Anthropocene, 3, https://doi.org/10.12952/journal.elementa.000038, 2015.

Moreau, S., Vancoppenolle, M., Delille, B., Tison, J.-L., Zhou, J., Kotovitch, M., Thomas, D.N., Geilfus, N.-X., and Goosse, H.: Drivers of inorganic carbon dynamics in first-year sea ice: A model study, J. Geophys. Rs. Oceans, 120, doi:10.1002/2014JC010388, 2015.

Moreau, S., Vancoppenolle, M., Bopp, L., Aumont, O., Madec, G., Delille, B., Tison, J.-L., Barriat, P.-780 Y., and Goosse, H.: Assessment of the sea-ice carbon pump: Insights from a three-dimensional ocean-sea-ice biogeochemical model (NEMO-LIM-PISCES), Elementa: Science of the Anthropocene, 4, https://doi.org/10.12952/journal.elementa.000122, 2016.

Mortenson, E., Steiner, N., Monahan, A. H., Miller, L. A., Geilfus, N.-X., and Brown, K.: A Model-Based Analysis of Physical and Biogeochemical Controls on Carbon Exchange in the Upper 785 Water Column, Sea Ice, and Atmosphere in a Seasonally Ice-Covered Arctic Strait, J. Geophys. Res. Oceans, 123, 7529–7549, https://doi.org/10.1029/2018JC014376, 2018.

Mundy, C. J., Barber, D. G., and Michel, C.: Variability of snow and ice thermal, physical and optical properties pertinent to sea ice algae biomass during spring, J. Mar. Sys., 58, 107–120, https://doi.org/10.1016/j.jmarsys.2005.07.003, 2005.

790 Nakawo, M. and Sinha, N. K.: Growth Rate and Salinity Profile of First-Year Sea Ice in the High Arctic, J. Glaciol., 27, 315–330, https://doi.org/10.3189/S0022143000015409, 1981.

Nomura, D., Yshikawa-Inoue, H., Toyota, T.: The effect of sea ice growth on air-sea CO2 flux in a tank experiment, Tellus B: Chemical and Physical Meteorology, 58(5) 418-426, 2006.

Nomura, D., Yoshikawa-Inoue, H., Toyota, T., Shirasawa, K.: Effects of snow, snowmelting and 795 refreezing processes on air-sea ice CO_2 flux, Journal of Glaciology, 56(196) 262-270, 2010.

Nomura, D., Yoshikawa-Inoue, H., Kobayashi, S., Nakaoka, S., Nakata, K., and Hashida, G.: Winter-to-summer evolution of pCO_2 in surface water and air–sea CO_2 flux in the seasonal ice zone of

the Southern Ocean, Biogeosciences, 11, 5749–5761, https://doi.org/10.5194/bg-11-5749-2014, 2014.

800   Notz, D. and Worster, M. G.: Desalination processes of sea ice revisited, J. Geophys. Res., 114, https://doi.org/10.1029/2008JC004885, 2009.

Parsons, T. R., Maita, Y., and Lalli, C. M.: A manual of chemical and biological methods for seawater analysis, New York: Pergamon Press, https://doi.org/10.1002/iroh.19850700634, 1984.

Petrich, C., and Eicken, H.: Growth, Structure and Properties of Sea Ice, in: Sea Ice, edited by:
805   Thomas, D.N., and Dieckmann, G.S., Jonn Wiley & Sons, United Kingdom, 23-79, 2010.

Provost, C., Sennéchael, N., Miguet, J., Itkin, P., Koenig, Z., Villacieros-Robineau, N., Granskog, M.A.: Observations of flooding and snow-ice formation in a thinner Arctic sea-ice regime during the N-ICE2015 campaign: Influence of basal ice melt and storms, J. Geophys. Res., 122(9), https://doi.org/10.1002/2016JC012011, 2017

810   Rysgaard, S. and Glud, R. N.: Anaerobic N_2 production in Arctic sea ice, Limnology and Oceanography, 49, 86–94, 2004.

Rysgaard, S., Glud, R. N., Sejr, M. K., Bendtsen, J., and Christensen, P. B.: Inorganic carbon transport during sea ice growth and decay: A carbon pump in polar seas, J. Geophys. Res., 112, https://doi.org/10.1029/2006JC003572, 2007.

815   Rysgaard, S., Bendtsen, J., Pedersen, L. T., Ramløv, H., and Glud, R. N.: Increased CO_2 uptake due to sea ice growth and decay in the Nordic Seas, J. Geophys. Res., 114, https://doi.org/10.1029/2008JC005088, 2009.

Rysgaard, S., Bendtsen, J., Delille, B., Dieckmann, G. S., Glud, R. N., Kennedy, H., Mortensen, J., Papadimitriou, S., Thomas, D. N., and Tison, J.-L.: Sea ice contribution to the air–sea CO_2
820   exchange in the Arctic and Southern Oceans, Tellus B, 63, 823–830, https://doi.org/10.1111/j.1600-0889.2011.00571.x, 2011.

Rysgaard, S., Søgaard, D. H., Cooper, M., Puc´ko M., Lennert, K., Papakyriakou, T. N., Wang, F., Geilfus, N. X., Glud, R. N., Ehn, J., McGinnis, D. F., Attard, K., Sievers, J., Deming, J. W., and Barber, D.: Ikaite crystal distribution in winter sea ice and implications for CO_2 system
825   dynamics, The Cryosphere, 7, 707–718, https://doi.org/10.5194/tc-7-707-2013, 2013.

Savel'yev, B. A.: Study of ice in the region of the drift of the station SP-4 during melt and breakup in 1955. *Problemy Severa 2,* 47-79, 1958.

Savel'yev, B. A.: Structure, composition and properties of the ice cover of sea and fresh waters, Moscow, Izdatel'stvo Moskovskogo Universiteta, 1963.

Spreen, G., Kaleschke, L., and Heygster, G.: Sea ice remote sensing using AMSR-E 89-GHz channels. J. Geophys. Res. Oceans, 113, C02S03, https://doi.org/10.1029/2005JC003384, 2008.

Takahashi, T., Sutherland, S. C., Wanninkhof, R., Sweeney, C., Feely, R. A., Chipman, D. W., Hales, B., Friederich, G., Chavez, F., Sabine, C., Watson, A., Bakker, D. C. E., Schuster, U., Metzl, N., Yoshikawa-Inoue, H., Ishii, M., Midorikawa, T., Nojiri, Y., Körtzinger, A., Steinhoff, T., Hoppema, M., Olafsson, J., Arnarson, T. S., Tilbrook, B., Johannessen, T., Olsen, A., Bellerby, R., Wong, C. S., Delille, B., Bates, N. R., and de Baar, H. J. W.: Climatological mean and decadal change in surface ocean pCO_2, and net sea–air CO_2 flux over the global oceans, Deep Sea Research Part II: Topical Studies in Oceanography, 56, 554–577, https://doi.org/10.1016/j.dsr2.2008.12.009, 2009.

Vancoppenolle, M., Fichefet, T., and Bitz, C. M.: Modeling the salinity profile of undeformed Arctic Sea ice, Geophys. Res. Lett., 33, https://doi.org/10.1029/2006GL028342, 2006.

Weeks, W. F. and Lee, O. S.: The Salinity Distribution in Young Sea-Ice, Arctic, 15, 92–108, https://doi.org/10.14430/arctic3562, 1962.

Weeks, W. F.: On Sea Ice, Fairbanks: University of Alaska Press. 49, 664p, ISBN 978-1-60223-079-8, 2010.

Welch, H. E., and Bergmann, M. A.: Seasonal development of ice algae and its prediction from environmental factors near Resolute, N.W.T., Canada. Can. J. Fish. Aquat. Sci., 46, 1793–1804, https://cdnsciencepub.com/doi/pdf/10.1139/f89-227, 1989.

Williams W. J., Brown, K. A., Bluhm, B. A., Carmack, E. C., Dalman, L., Danielson, S. L., Else, B. G. T., Fredriksen, R., Mundy, C. J., Rotermund, L. M., and Schimnowski, A.: Stratification in the Canadian Arctic Archipelago's Kitikmeot Sea: biological and geochemical consequences, Polar Knowledge, Aqhaliat 2018, Polar Knowledge Canada, 46–52, DOI: 10.35298/pkc.2018.06, 2018.

Xu, C., Mikhael, W., Myers, P. G., Else, B., Sims, R. P., and Zhou, Q.: Effects of seasonal ice coverage on the physical oceanographic conditions of the Kitikmeot Sea in the Canadian Arctic Archipelago, Atmosphere-Ocean, https://doi.org/10.1080/07055900.2021.1965531, 31 August 2021.

Yasunaka, S., Murata, A., Watanabe, E., Chierici, M., Fransson, A., Heuven, S. van, Hoppema, M., Ishii, M., and Johannssen, T., Kosugi, N., Lauvset, S. K., Mathis, J. T., Nishino, S., Omar, A. M., Olsen, A., Sasano, D., Takahashi, T., and Wanninkhof, R.: Mapping of the air–sea CO_2 flux in the Arctic Ocean and its adjacent seas: Basin-wide distribution and seasonal to interannual variability, Polar Science, 10, 323–334, https://doi.org/10.1016/j.polar.2016.03.006, 2016.

Table 1: Mean (x), standard deviation (σ) and range (max-min) of the measured physical and biological conditions at the two sampling sites. Sample size for snow depth and ice thickness was $n=15$, except for TFYI ice thickness ($n=14$). Sample size for Chl a was $n=3$, therefore standard deviation is not displayed.

870

	Thick FYI (TFYI)				Polynya (POLY)			
	Snow Depth (cm)	Ice Thickness (cm)	Current Velocity (cm/s)	Bottom Chl a (mg/m^2)	Snow Depth (cm)	Ice Thickness (cm)	Current Velocity (cm/s)	Bottom Chl a (mg/m^2)
$\overline{x}$	15.0	180.5	1.4	14.2	26.0	146.8	9.5	4.3
σ	4.8	8.9	0.6		7.9	16.2	9.5	
range	8.0 - 25.0	161 - 191	0.5 - 4.3	11.3 - 16.1	9.5 - 26.0	124 - 174	0.0 - 44.8	2.6 - 5.6

Table 2: Summary of biogeochemical variables measured at the two sites, across the three horizons. Mean (x) and standard deviation (σ) are presented. Sample depth is the mid-point of the core sections collected for each horizon. For each horizon, at each site, $n=15$.

875

			Thick FYI (TFYI)					Polynya (POLY)				
			Sample Depth (cm)	Salinity (PSU)	TIC (µmol kg^{-1})	TA (µmol kg^{-1})	TA:TIC	Sample Depth (cm)	Salinity (PSU)	TIC (µmol kg^{-1})	TA (µmol kg^{-1})	TA:TIC
HORIZON	Top	$\overline{x}$	5	5.43	281.63	333.24	1.18	5	6.79	343.33	403.56	1.17
		σ	0	0.42	21.98	30.16	0.05	0	1.18	61.83	78.13	0.05
	Middle	$\overline{x}$	89	4.63	331.55	345.91	1.05	73	4.88	341.89	363.22	1.06
		σ	4	0.46	29.77	31.39	0.03	8	0.90	34.60	40.88	0.04
	Bottom	$\overline{x}$	176	7.89	538.37	551.60	1.02	142	6.73	450.93	478.71	1.06
		σ	9	0.39	20.55	26.08	0.02	16	0.71	52.45	51.65	0.03

885 **Table 3:** Results of the ANOVA analysis for parameters measured at the two sites. Shaded cells indicate a statistically significant (p<0.01) difference in the mean value between the two sites.

		Variable Tested	ANOVA p-value
		Snow Depth	<0.001
		Ice Thickness	<0.001
HORIZON	Top	Salinity	<0.001
		TIC	0.001
		TA	0.003
		TA:TIC	0.544
	Middle	Salinity	0.339
		TIC	0.388
		TA	0.218
		TA:TIC	0.252
	Bottom	Salinity	<0.001
		TIC	<0.001
		TA	<0.001
		TA:TIC	0.001

Table 4: Slope values of sTA/sTIC (i.e. Figure 8) for each of the horizons at each site, and for all samples at each site. Also reported is the r^2 value for each regression line, as well as the p-value testing
890 the significance of each slope.

		Thick FYI (TFYI)			Polynya (POLY)		
		Slope	r^2	p value	Slope	r^2	p value
HORIZON	Top	0.96	0.79	<0.01	1.03	0.91	<0.01
	Middle	0.37	0.39	0.01	0.87	0.86	<0.01
	Bottom	0.67	0.46	<0.01	0.50	0.48	<0.01
	All	0.65	0.88	<0.01	0.81	0.95	<0.01

895

Table 5: Vertically weighted average TIC and TA for the two sites. Weighting calculated attributing top and bottom horizon values (Table 2) to the surface and bottom 10cm of ice, and the middle horizon values to the mean ice thickness subtracting the 20 cm accounted for by the top and bottom measurements.

	TIC (μmol kg^{-1})	TA (μmol kg^{-1})	TA:TIC
TFYI	340.24	356.60	1.05
POLY	349.42	373.84	1.07
Difference	2.6%	4.6%	2.0%
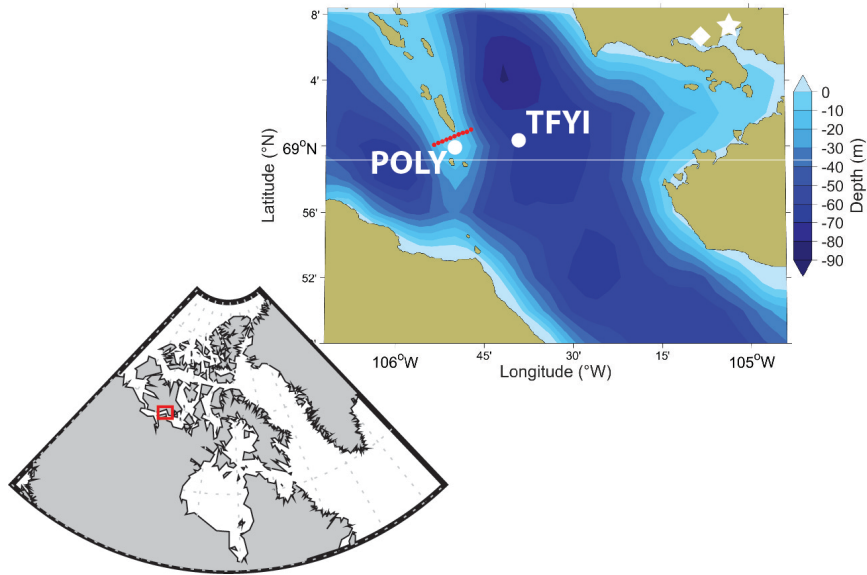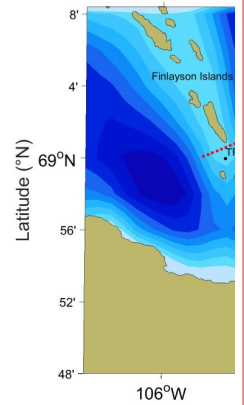
900

Figure 1: Study area (including bathymetry), showing the location of the two sampling sites. The thick first year ice site (TFYI) was located at 69.01°N, 105.66°W. The polynya site (POLY) was located at 68.99°N, 105.84°W. The proximity to Cambridge Bay (white star), the nearest Environment Canada weather station (white diamond), and the snow depth/ice thickness transect (red circles) is also shown.

915
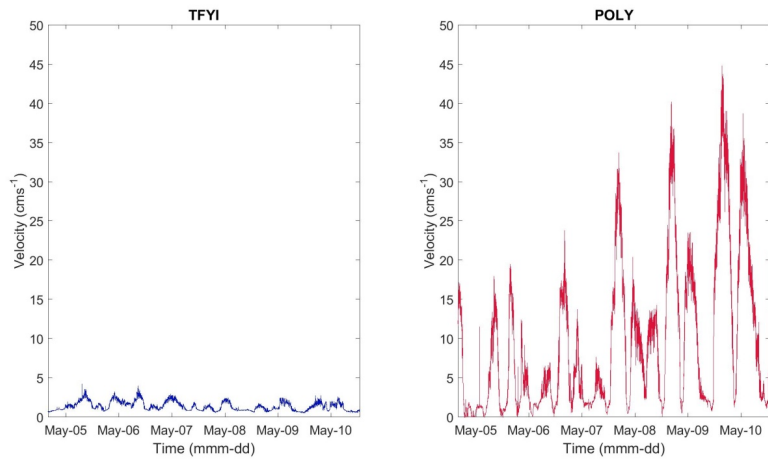
Figure 2: Under ice current velocities observed at the two sites during the sampling period.
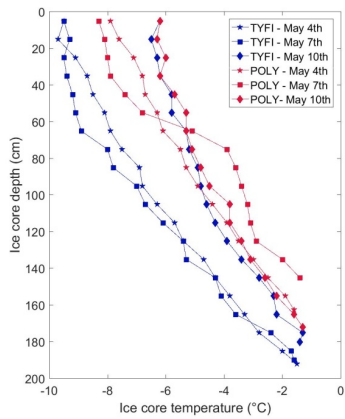
920 **Figure 3: Ice temperature profiles at both sites, from each of the daily temperature/salinity cores.**
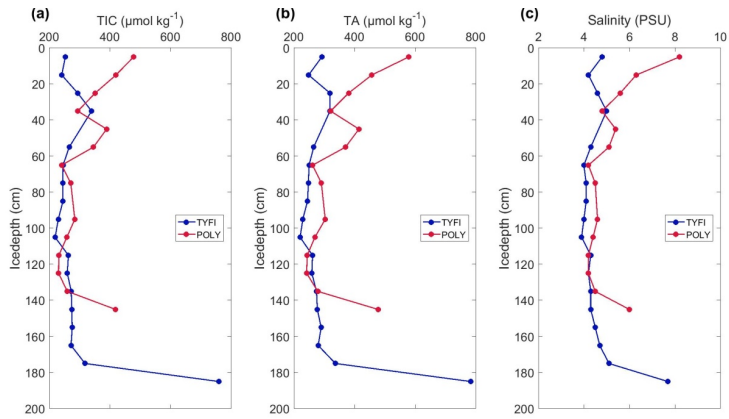
Figure 4: TIC (panel a), TA (panel b) and salinity (panel c) results of the high resolution (10-cm interval) cores collected on the final sampling day.
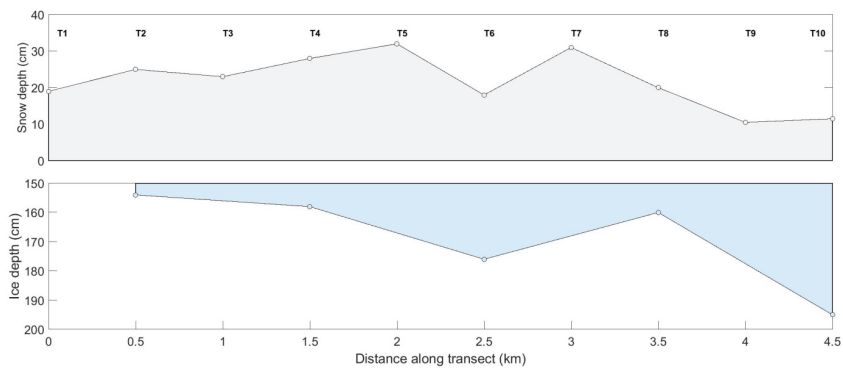
930   **Figure 5: Results of the snow depth and ice thickness survey conducted just north of our sampling**
sites on 12 May.
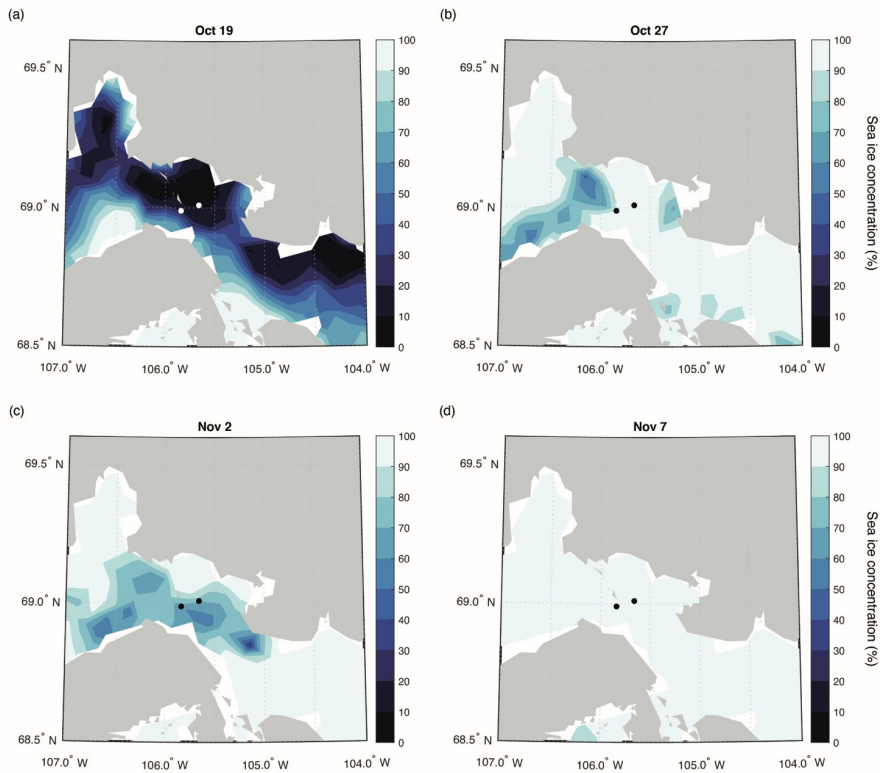
935

Figure 6: Sea ice concentration of the study area during sea ice freeze-up on (a) 19 October, (b) 27 October, (c) 2 November, and (d) 7 November 2018. The sampling sites are noted (see also Figure 1) with black or white dots depending on contrast.
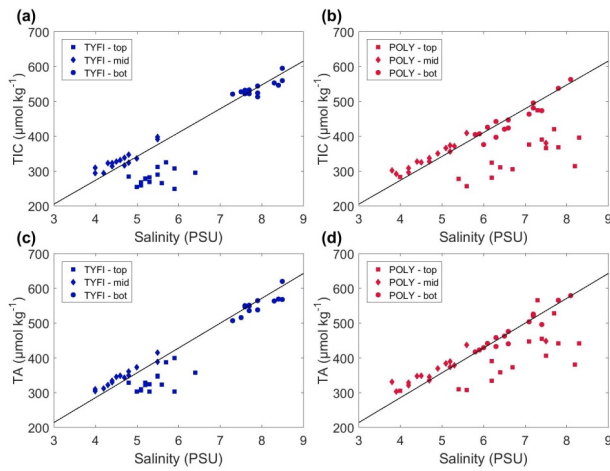
Figure 7: **Bulk sea ice TIC and TA from the statistical samples (i.e. top, middle, bottom)** plotted

against bulk salinity for both sites **and on all dates. The solid line is the slope of a theoretical mixing**

line between a pure ice endmember (S, TIC, TA = 0) and a source seawater endmember (S_{ref} = 28.8,

TA_{ref} = 2058 mmol kg^{-1}, TIC_{ref} = 1970 mmol kg^{-1}),

Deleted: Bulk Sea ice TIC and TA

Deleted: .
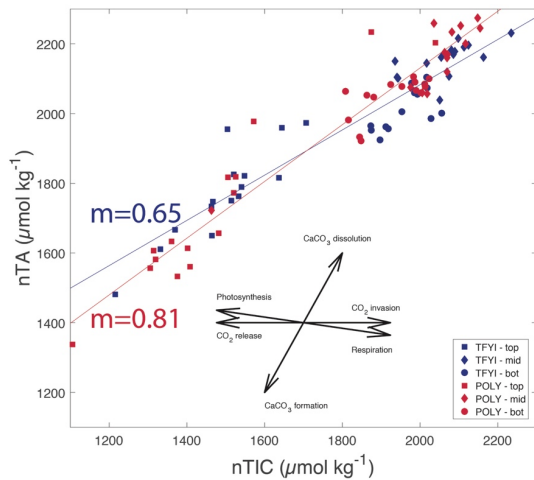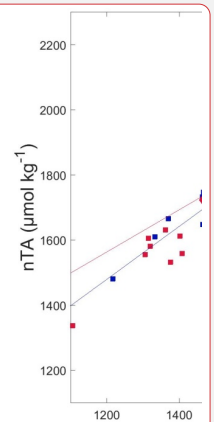
Figure 8: Normalized bulk TIC (nTIC) plotted against normalized bulk TA (nTA). Solid lines are the regression relationship for all TFYI statistical samples (slope noted with blue text) and for all POLY statistical samples (slope noted with red text). The rosette diagram shows the theoretical slopes that would occur if only one process was occurring: photosynthesis/respiration (nTA/nDIC = 17/106), CaCO$_3$ dissolution/formation (nTA/nDIC = 2/1), and gas exchange (nTA/nDIC = 1/1).